# Automatic Heart Localization and Radiographic Index Computation in Chest X-rays

Sema Candemir, Stefan Jaeger, Wilson Lin,* Zhiyun Xue, Sameer Antani, George Thoma

National Library of Medicine, National Institutes of Health, Bethesda, MD, USA

## ABSTRACT

This study proposes a novel automated method for cardiomegaly detection in chest X-rays (CXRs). The algorithm has two main stages: i) heart and lung region localization on CXRs, and ii) radiographic index extraction from the heart and lung boundaries. We employed a lung detection algorithm and extended it to automatically compute the heart boundaries. The typical models of heart and lung regions are learned using a public CXR dataset with boundary markings. The method estimates the location of these regions in candidate ('patient') CXR images by registering models to the patient CXR. For the radiographic index computation, we implemented the traditional and recently published indexes in the literature. The method is tested on a database with 250 abnormal, and 250 normal CXRs. The radiographic indexes are combined through a classifier, and the method successfully classifies the patients with cardiomegaly with a 0.77 accuracy, 0.77 sensitivity and 0.76 specificity.

**Keywords:** Chest X-rays, Cardiomegaly, Radiographic index, Lung boundary, Heart boundary

## 1. INTRODUCTION

Chest radiography is commonly used as an early diagnosis tool to observe/detect the lung and heart pathologies such as atelectasis, consolidation, pneumothorax, pleural/pericardial effusion, cardiac hypertrophy/hyperinflation[1] and is a primary tool for mass screening.[2,3] It is accessible, inexpensive and dose-effective compared to other imaging tools. The literature has many studies for automated analysis of chest X-rays (CXR) to assist radiologists by reducing their efforts during the analysis, or for mass population screening in endemic locations.[2–4] One of these attempts is computation of radiographic indexes from CXRs, and using them as an indicator for cardiac diseases such as cardiomegaly (enlarged heart).

In this study, we propose a novel automated method to locate the boundaries of heart and the lung, and compute the radiographic indexes from the boundaries. We do a comparative study of the performance of radiographic indexes for cardiomegaly detection. We also combine the indexes in order to improve the algorithm performance. Our contributions are i) a new approach to detect the cardiac boundary, ii) a fully automated method to extract the radiographic indexes, and iii) a comparison of index performance on a large dataset. We believe that our efforts will be useful for developing a screening system for heart enlargement detection on CXRs.

## 2. LITERATURE

MacMahon et al.[5] recorded 1089 CXRs, and observed the abnormalities. They found that 27% of CXRs have abnormalities of heart size which ranked third among all abnormalities. In a recent study, Demner-Fushman et al. prepared a publicly available collection of CXRs. In the collection, among 2470 abnormal CXRs, 375 (15.1 %) have cardiomegaly, ranked first among all abnormalities.[6] These high numbers lead us to seek automatic ways to analyze the heart size, compute the radiographic indexes and develop a screening system for cardiomegaly detection.

Several studies for detection of heart diseases from CXRs have been reported in the literature. The well-known measurement is cardiothoracic ratio (CTR) which is defined as the ratio between the maximum transverse cardiac diameter and the maximum thoracic diameter measured between the inner margins of ribs (c.f. Section 3.2).

---

* Wilson Lin is a student at University of Maryland, College Park, MD, USA. He contributed to this work during his summer fellowship at NLM.
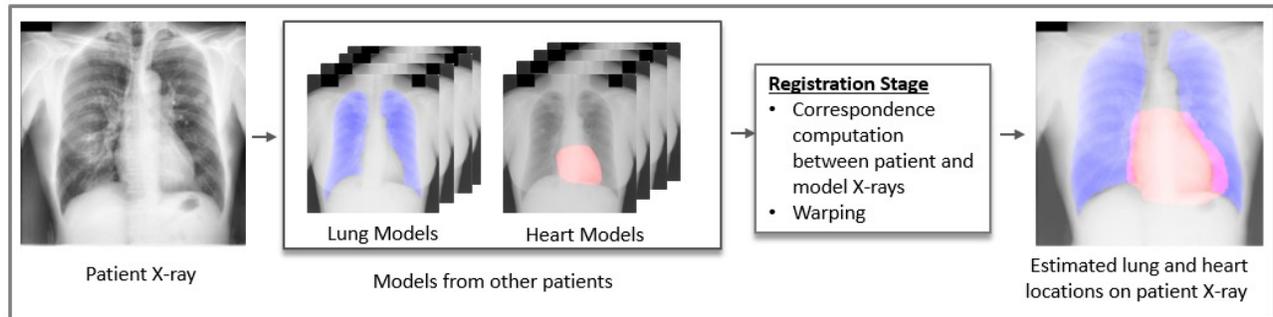 Send correspondence to sema.candemir@nih.gov

Figure 1. Flowchart of the boundary detection algorithm

It was first proposed in 1919 to screen military recruits.[7] In one of the first automated systems,[8] the authors developed an analytical program which measured the maximum diameter of the heart shadow and the maximum diameter of the rib-cage shadow from CXRs using vertical intensity histogram analysis. Another automated computation of CTR is proposed in[9] and then in[10] by fitting a Fourier shape to heart boundary profiles. In[11] the authors proposed boundary extraction methods for lung, clavicle, and heart regions. As an application, the cardiothoracic ratio is computed from the boundary results. In[12] the lung area is detected with local shape and patient-specific shape models, and CTR is computed from the lung boundaries. Although the traditional CTR is widely accepted as a standard index for heart analysis in CXRs, the literature shows research toward other radiographic indexes. In[13] CTR is defined as the ratio between the pixel counts of the cardiac outline and the whole thorax. It is computed from the borders of lung and heart; therefore, researchers named this radiographic index 2D-CTR. The automatic computation of this measure is proposed in.[14] In[15] another 2D-CTR is defined as the square root of the ratio between the cardiac area and the thorax area. The relationship between the traditional and 2D-CTR are measured, and it is found that 2D-CTR is highly correlated with the traditional CTR. In[14] the ratio of the area of heart region to the area of lung region (CTAR) is proposed as an index. The authors claimed that area ratio provides higher discrimination power than the 2D-CTR and 1D-CTR indexes for detecting heart enlargement.

## 3. AUTOMATIC LOCALIZATION OF HEART/LUNG SHADOWS AND RADIOGRAPHIC INDEX COMPUTATION

### 3.1 Automatic Localization of Heart and Lung Shadows

The boundary detection stage of our method is based on our previous work on lung boundary detection.[4,16] We extend this work to automatically detect the heart location. The flowchart of the algorithm is illustrated in Figure 1.

The method uses existing CXRs and their radiologist marked lung/heart boundaries as models, and estimates the lung/heart boundary of a patient X-ray by registering the model X-rays to the patient X-ray. We use a public CXR dataset[17] (c.f. section 4.1) with reference boundaries.[11] When a patient X-ray is presented, the method first finds the most similar X-rays in the model set to the patient X-ray. The similarity between X-rays is measured by comparing the horizontal and vertical intensity histograms of X-rays. We use the Bhattacharyya distance as a similarity index. The most similar X-rays will register to the patient's X-ray in the next stage. The main purpose of measuring the similarity is to increase the correspondence performance and decrease the computational expense during registration. After the model selection, we compute the correspondence map between the model X-ray and patient X-ray. The correspondence map computation is conducted by modeling the patient X-ray with local image features, and matching the most similar locations. For the correspondence map computation, we employ the SIFT-flow algorithm.[18] The computed map is considered to be a transformation from model X-rays to the patient X-ray. The transformation matrix is applied to the model masks to transform them into the approximate lung/heart model for the patient X-ray. The performance of the heart and lung localization is presented in the experimental section (c.f. Section 4).
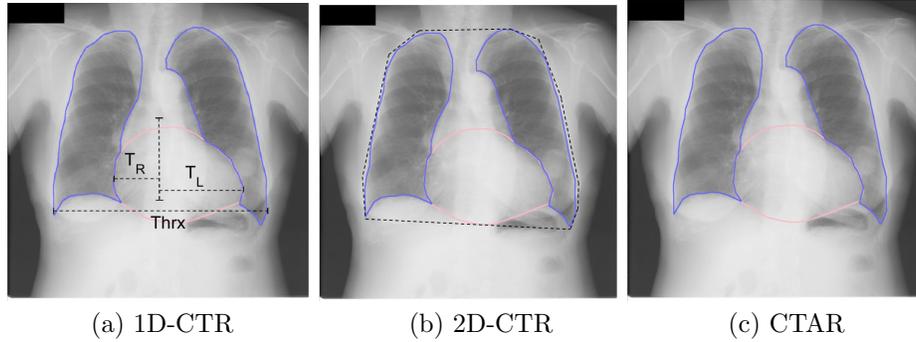
(a) 1D-CTR          (b) 2D-CTR          (c) CTAR

Figure 2. Illustration of radiographic indexes on CXRs.

## 3.2 Radiographic Indexes

After locating the heart and lung regions, we automatically compute the following indexes from the boundaries.

**1D-CTR:** is the traditional cardiothoracic ratio (CTR), and is defined as the ratio between the maximum transverse cardiac diameter and the maximum thoracic diameter measured between the inner margins of ribs.[7, 13, 19, 20] Figure 2.(a) illustrates 1D-CTR which is computed as follows,

$$\text{CTR} = \frac{\text{T}_L + \text{T}_R}{\text{Thrx}} \tag{1}$$

where $\text{T}_L$ is the transverse left heart diameter, $\text{T}_R$ is the transverse right heart diameter, and Thrx is the diameter of the thorax. We assume that the largest outer distance from one lung lobe to other lobe corresponds to the horizontal diameter of thorax (Thrx). For the transverse diameter computation, we first compute the spine line with profile analysis. The maximum peak in the center of the vertical profile histogram corresponds to the spine line. We define the largest inner distance from the left lobe to the spine line as the left transverse diameter ($\text{T}_L$), and the largest inner distance from the right lobe to the spine line as the right transverse diameter ($\text{T}_R$). Although there is no consensus on the optimal CTR for cardiomegaly,[21, 22] CTR higher than 0.5 is considered as cardiac enlargement[23] as a sign of cardiomegaly, pericardial effusion, anterior mediastinal mass, or prominent epicardial fat pad.[24]

**2D-CTR** is defined as the ratio between the boundary perimeter of the heart region and the boundary perimeter of the entire thoracic region.[13] The thoracic boundary is computed by applying the convex hull to the lung regions. The radiographic index is illustrated in Figure 2(b) and formulated as follows,

$$\text{2D-CTR} = \frac{\text{Perimeter(H)}}{\text{Perimeter(Thrx)}} \tag{2}$$

It is claimed[13] that 2D-CTR is more correlated with cardiac functions and more robust than 1D-CTR. The ratio 0.23 or higher is considered as abnormal.

**CTAR - Cardiothoracic area ratio** is the ratio of the area of heart region to the area of lung region.[14] The index computation is illustrated in Figure 2(c) and formulated as follows,

$$\text{CTAR} = \frac{\text{Area(H)}}{\text{Area}(\text{L}_R) + \text{Area}(L_L)} \tag{3}$$

where $L_R$ and $L_L$ are the right and left lung region, respectively. According to[14] healthy persons have a CTAR value of 0.41 or less.

# 4. EXPERIMENTS

## 4.1 Data Set and Validation

We test the algorithm with the following datasets:

**JSRT Set**[17] is compiled by the Japanese Society of Radiological Technology (JSRT). The set contains 247 CXRs, among which 154 have lung nodules, and 93 have no nodules. All x-ray images have a size of $2048 \times 2048$ pixels and a gray-scale color depth of 12 bit. The pixel spacing in vertical and horizontal directions is 0.175mm. The set is publicly available and has gold standard boundaries[11] for performance evaluation. In our experiments, we use the boundaries in the JSRT dataset as training masks for the registration stage. The set is publicly available[25] with the reference heart and lung boundaries (SCR database).[11,26]

**Indiana Set**[6] is a set collected from various hospitals affiliated with the Indiana University School of Medicine. The set contains approximately 4000 frontal and lateral CXRs with several lung abnormalities. From these, we selected 250 frontal CXRs which contain cardiomegaly with various levels such as borderline, mild, and severe. We also selected 250 CXR among the normal cases for testing. The set is publicly available through Open-i$^{\text{SM}}$,[27] which is a multimodel (image + text) biomedical literature search engine developed by U.S. National Library of Medicine.

**Evaluation:** We used overlap $= |TP|/(|FP| + |TP| + |FN|)$ measure for boundary detection performance, where TP (true positive) represents correctly classified pixel, FP (false positives) represents pixels that are classified as heart or lung, but that are in fact background, and FN (false negatives) represents pixels that are classified as background that are in fact part of the heart or lung region. The classification performance of CXRs with radiographic indexes are measured with accuracy $= (|TP| + |TN|)/(|TP| + |TN| + |FP| + |FN|)$, sensitivity $= |TP|/(|TP| + |FN|)$ and specificity $= |TN|/(|TN| + |FP|)$. In this case, TP represents correctly classified CXRs, FP are the healthy CXRs that have been classified as abnormal, and FN are the abnormal CXRs that have been classified as normal.

## 4.2 Automatic Localization of Heart and Lung Shadows

We built a test-bed system as described in Section 3.(A) and locate the lung and heart regions. The results are reported in Table 1. Figure 3 shows examples of segmentation results.

|  | Overlap Measure (Heart boundary) |
|---|---|
| Human Observer[11] | $0.878 \pm 0.054$ |
| Model-based | $0.697 \pm 0.087$ |

|  | Overlap Measure (Lung boundary) |
|---|---|
| Human Observer[11] | $0.946 \pm 0.018$ |
| Model-based[4] | $0.954 \pm 0.002$ |

Table 1. Average overlap value for heart and lung boundary in JSRT set.



Figure 3. Example segmentation results for lung and cardiac regions.

| Variable | Normal Cases (mean ± stdv) | Cardiomegaly Cases (mean ± stdv) |
|---|---|---|
| $T_R$ (cm) | 6.02 ± 2.41 | 6.41 ± 2.11 |
| $T_L$ (cm) | 9.27 ± 1.46 | 10.5 ± 2.04 |
| 1D-CTR (%) | 49.9 ± 7.60 | 56.5 ± 7.10 |
| 2D-CTR (%) | 57.1 ± 8.50 | 65.4 ± 11.1 |
| CTAR (%) | 57.9 ± 17.8 | 82.1 ± 28.6 |

Table 2. Average radiographic measurements for normal CXRs and cardiomegaly CXRs. Each set has 250 CXRs.

## 4.3 Extracting radiographic indexes

Based on the lung and heart boundary results, we compute the radiographic indexes on normal and abnormal cases. Table 2 shows the average radiographic measurements.

Although the literature defined decision thresholds for 1D-CTR, 2D-CTR and CTAR, our automated system did not produce adequate classification results with these thresholds. In order to find the optimal thresholds (decision line), we compute the Receiver Operating Characteristic (ROC) curves for each radiographic index. Figure 4 shows the ROC curves. We found that the optimal decision line for 1D-CTR is 0.514, for 2D-CTR is 0.591 and for CTAR is 0.626.
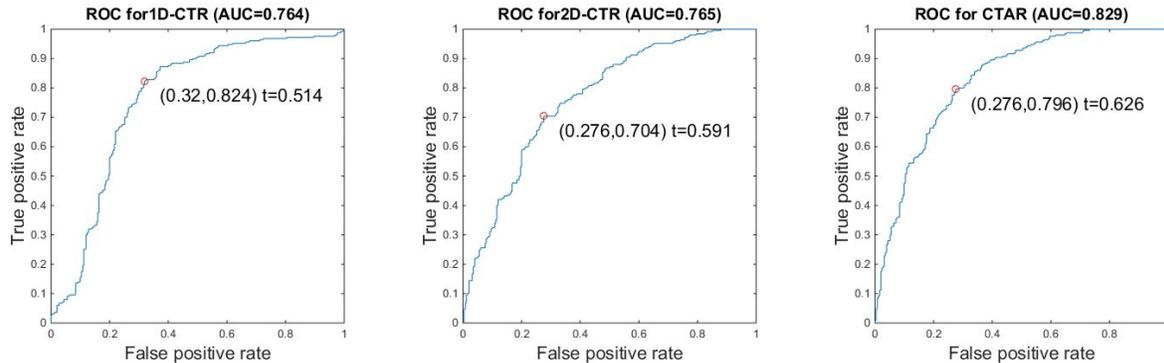


Figure 4. Receiver Operating Characteristic curves and optimal threshold value for abnormality decision for each radiographic index.

We measured the system performance in terms of accuracy, sensitivity and specificity with the optimal decision points. If the radiographic index is higher than the optimal threshold, then the CXR is classified as abnormal (cardiomegaly). The results are summarized in Table 3 and the scatterplots with the decision lines are shown in Figure 5.

| | Accuracy | Sensitivity | Specificity |
|---|---|---|---|
| 1D-CTR | 0.736 | 0.872 | 0.60 |
| 2D-CTR | 0.708 | 0.704 | 0.712 |
| CTAR | 0.756 | **0.856** | 0.656 |
| Classifier | **0.765** | 0.771 | **0.764** |

Table 3. The performance of the radiographic indexes with respect to optimal decision line.

In order to increase the system performance, we combined the radiographic indexes via a classifier. We follow the Monte Carlo cross-validation, and randomly partition the data into training (80%) and test set (20%). As a classifier, we employ support vector machine (SVM). All indexes for the test set are entered in SVM, and the trained system classifies the patient X-ray as cardiomegaly, or non-cardiomegaly. The experiment is repeated 100 times with randomly partitioned training and test sets. The average accuracy, sensitivity, and specificity scores are reported in Table 3, in the last row. The flowchart of this stage is illustrated in Figure 6.
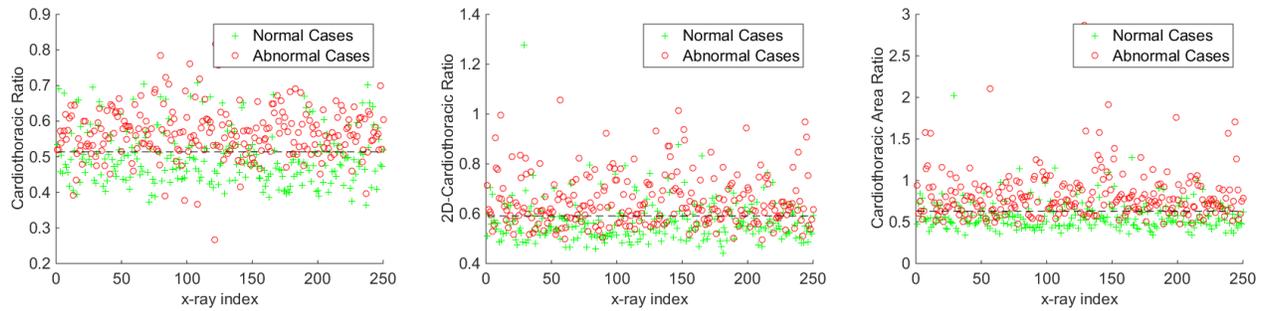
Figure 5. The scatterplots with decision threshold. The red circles represent the abnormal, the green plus signs represent the normal CXRs.
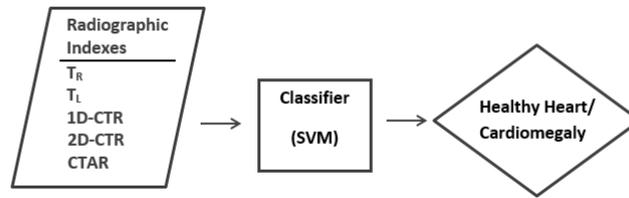


Figure 6. A simple flowchart for combination of radiographic indexes

## 5. CONCLUSIONS

In this study, we presented a novel automated method to detect cardiomegaly in CXRs. The system first locates the heart and lung regions in CXRs, and then extracts the radiographic indexes from the boundaries. According to our experiments, CTAR provides slightly higher discrimination power than the other indexes, 1D-CTR and 2D-CTR. The combined indexes produce slightly higher accuracy and specificity than each individual index.

The accuracy of radiographic indexes is directly affected by the accuracy of the boundary detection stage. Our algorithm produces state-of-the-art performance on lung region detection, and provides comprable annotation to a human observer.[4, 16] However, the segmentation of the heart is more difficult than the lung region detection, since the upper and lower parts of the heart boundary are not clearly visible in CXRs. The literature studies[11] also reported lower boundary detection accuracy for heart boundaries. With a better heart localization approach, the radiographic index extraction and abnormality classification stages could be improved.

Some studies have questioned the effectiveness of CTR for cardiomegaly detection. For example, in[28] and in,[29] CTR is compared with 2D-echocardiography, which is the current gold standard for the diagnosis of cardiomegaly, and concluded that the results are correlated. On the other hand, in[13, 30–32] CTR did not perform as well as echocardiography. The main reasons for low accuracy of radiographic indexes are due to fact that the cardiac size and the width of thorax are affected by respiration, the cardiac cycle phase, heart rate at the time of examination, and pathologic conditions such as emphysema.[32] All these external parameters could affect the CTR measurement, and so chest radiography could only provide a rough estimate of cardiac and thorax size.[33] By analyzing our results, we can conclude that due to routine availability of CXRs and the easy computation of radiographic indexes, an automatic screening system could be useful for the early detection of heart enlargement.

## ACKNOWLEDGMENT

## REFERENCES

[1] Corne, J. and Pointon, K., [*Chest X-Ray Made Easy*], Churchill Livingstone; 3 edition (2009).
[2] "National library of medicine, chest x-ray screening project." http://archive.nlm.nih.gov/repos/chestImages.php/. [Online; accessed 24-August-2015].

[3] Jaeger, S., Karargyris, A., Candemir, S., Folio, L., Sielgelman, J., Callaghan, F., Xue, Z., Palaniappan, K., Singh, R., Antani, S., Thoma, G., Xiang, Y.-X., Lu, P.-X., and McDonald, C., "Automatic tuberculosis screening using chest radiographs," *IEEE Trans. on Medical Imaging* **33**(2), 233–245 (2014).

[4] Candemir, S., Jaeger, S., Palaniappan, K., J.P., M., R.K., S., Xue, Z., Karargyris, A., Antani, S., Thoma, G., and McDonald, C., "Lung segmentation in chest radiographs using anatomical atlases with non-rigid registration," *IEEE Trans. on Medical Imaging* **33**(2), 577–590 (2014).

[5] MacMahon, H., Liu, K., Montner, S., and Doi, K., "The nature and subtlety of abnormal findings in chest radiographs," *Med Phys.* **18**(2), 206–210 (1991).

[6] Demner-Fushman, D., Kohli, M. D., Rosenman, M. B., Shooshan, S. E., Rodriguez, L., Antani, S., Thoma, G. R., and McDonald, C. J., "Preparing a collection of radiology examinations for distribution and retrieval," *Journal of the American Medical Informatics Association* (2015).

[7] Danzer, C. S., "The cardiothoracic ratio: an index of cardiac enlargement.," *The American Journal of the Medical Sciences* **157**(4), 513–554 (1919).

[8] Becker, H., Nettleton Jr, W., Meyers, P., Sweeney, J., and Nice Jr, C., "Digital computer determination of a medical diagnostic index directly from chest x-ray images," *Biomedical Engineering, IEEE Transactions on* (3), 67–72 (1964).

[9] Nakamori, N., Doi, K., Sabeti, V., and MacMahon, H., "Image feature analysis and computer-aided diagnosis in digital radiography: automated analysis of sizes of heart and lung in chest images," *Medical Physics* **17**(3), 342–350 (1990).

[10] Nakamori, N., Doi, K., MacMahon, H., Sasaki, Y., and Montner, S., "Effect of heart-size parameters computed from digital chest radiographs on detection of cardiomegaly: potential usefulness for computer-aided diagnosis," *Investigative Radiology* **26**(6), 546–550 (1991).

[11] van Ginneken, B., Stegmann, M., and Loog, M., "Segmentation of anatomical structures in chest radiographs using supervised methods: a comparative study on a public database," *Medical Image Analysis* **10**(1), 19–40 (2006).

[12] Seghers, D., Loeckx, D., Maes, F., Vandermeulen, D., and Suetens, P., "Minimal shape and intensity cost path segmentation," *Medical Imaging, IEEE Transactions on* **26**(8), 1115–1129 (2007).

[13] Browne, R., OReilly, G., and McInerney, D., "Extraction of the two-dimensional cardiothoracic ratio from digital pa chest radiographs: correlation with cardiac function and the traditional cardiothoracic ratio," *Journal of digital imaging* **17**(2), 120–123 (2004).

[14] Hasan, M., Lee, S., Kim, D., and Lim, M., "Automatic evaluation of cardiac hypertrophy using cardio-thoracic area ratio in chest radiograph images," *Computer methods and programs in biomedicine* **105**(2), 95–108 (2012).

[15] Shi, Y., Qi, F., Xue, Z., Chen, L., Ito, K., Matsuo, H., and Shen, D., "Segmenting lung fields in serial chest radiographs using both population-based and patient-specific shape statistics," *Medical Imaging, IEEE Transactions on* **27**(4), 481–494 (2008).

[16] Candemir, S., Jaeger, S., Palaniappan, K., Antani, S., and Thoma, G., "Graph cut based automatic lung boundary detection in chest radiographs," *IEEE Healthcare Innovation Conference* (2012).

[17] Shiraishi, J., Katsuragawa, S., Ikezoe, J., Matsumoto, T., Kobayashi, T., Komatsu, K., Matsui, M., Fujita, H., Kodera, Y., and Doi, K., "Development of a digital image database for chest radiographs with and without a lung nodule: receiver operating characteristic analysis of radiologists detection of pulmonary nodules," *American Journal of Roentgenology* **174**, 71–74 (2000).

[18] Liu, C., Yuen, J., and Torralba, A., "SIFT flow: Dense correspondence across different scenes and its applications.," *IEEE Trans. Pattern Anal. Mach. Intell.* **33**(5) (2011).

[19] Becker, H., Nettleton, W., Meyers, P., Sweeney, J., and Nice, C., "Digital computer determination of a medical diagnostic index directly from chest x-ray images," *IEEE Trans. Biomed. Eng.* **11**, 67–72 (1964).

[20] Meyers, P., Nice, C., Becker, H., Nettleton, W., Sweeney, J., and Meckstroth, G., "Automated computer analysis of radiographic images," *Radiology* **83**, 1029–1034 (1964).

[21] Edwards, D., Higgins, C. B., and Gilpin, E., "The cardiothoracic ratio in newborn infants," *American Journal of Roentgenology* **136**(5), 907–913 (1981).

[22] Esguerra Gómez, G., "Importance of the relation between the anthropometric index and the transverse cardiac diameter for appraising the size of the heart 1," *Radiology* **57**(2), 217–226 (1951).

[23] Frishman, W. H., Nadelmann, J., Ooi, W. L., Greenberg, S., Heiman, M., Kahn, S., Guzik, H., Lazar, E. J., and Aronson, M., "Cardiomegaly on chest x-ray: prognostic implications from a ten-year cohort study of elderly subjects: a report from the bronx longitudinal aging study," *American heart journal* **124**(4), 1026–1030 (1992).

[24] Kearney, M., Nolan, J., Lee, A., Brooksby, P., Prescott, R., Shah, A., Zaman, A., Eckberg, D., Lindsay, H., and Batin, P., "A prognostic index to predict long-term mortality in patients with mild to moderate chronic heart failure stabilised on angiotensin converting enzyme inhibitors," *European Journal of Heart Failure* **5**(4), 489–497 (2003).

[25] "JSRT digital image database." http://www.jsrt.or.jp/jsrt-db/eng.php. [Online; accessed 29-January-2016].

[26] "SCR reference lung boundaries." http://www.isi.uu.nl. [Online; accessed 29-January-2016].

[27] "National library of medicine, open-i project." https://openi.nlm.nih.gov//. [Online; accessed 29-January-2016].

[28] Sinha, U., Sahay, U., Athavale, S., Deopujari, R., and Kumar, S., "Comparative study of cardiac size by chest x-ray and echocardiography," *Journal of the Anatomical Society of India* **62**(1), 28 – 32 (2013).

[29] Monfared, A. B., Farajollah, S. A., Sabour, F., Farzanegan, R., and Taghdisi, S., "Comparison of radiological findings of chest x-ray with echocardiography in determination of the heart size," (2015).

[30] Dinsmore, R. E., Goodman, D. J., and Sanders, C. A., "Some pitfalls in the evaluation of cardiac chamber enlargement on chest roentgenograms 1," *Radiology* **87**(2), 267–273 (1966).

[31] Philbin, E., Garg, R., Danisa, K., Denny, D., Gosselin, G., Hassapoyannes, C., Horney, A., Johnstone, D., Lang, R., Ramanathan, K., et al., "The relationship between cardiothoracic ratio and left ventricular ejection fraction in congestive heart failure," *Archives of internal medicine* **158**(5), 501–506 (1998).

[32] Clark, A. L. and Coats, A. J., "Unreliability of cardiothoracic ratio as a marker of left ventricular impairment: comparison with radionuclide ventriculography and echocardiography," *Postgraduate medical journal* **76**(895), 289–291 (2000).

[33] Ghali, J. K., Liao, Y., Simmons, B., Castaner, A., Cao, G., and Cooper, R. S., "The prognostic role of left ventricular hypertrophy in patients with or without coronary artery disease," *Annals of Internal Medicine* **117**(10), 831–836 (1992).